

AD-A046 231

ROME AIR DEVELOPMENT CENTER GRIFFISS AFB N Y
DIAGNOSTIC USE OF LIQUID CRYSTAL DETECTORS IN MICROSTRIP ANTENN--ETC(U)

F/G 9/1

JUL 77 J MCILVENNA, N KERNWEIS

UNCLASSIFIED

RADC-TR-77-250

NL

| OF |
AD
A046231



END
DATE
FILED
12-77
DDC

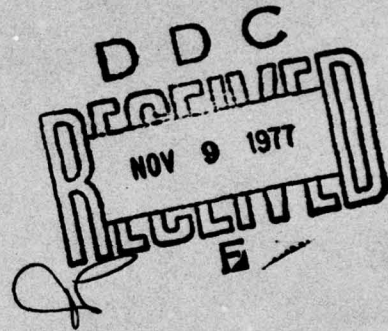
ADA046231

RADC-TR-77-250
IN-HOUSE REPORT
JULY 1977



Diagnostic Use of Liquid Crystal Detectors in Microstrip Antenna Design

JOHN McILVENNA
NICHOLAS KERNWEIS



RU NW.
DDC FILE COPY

Approved for public release; distribution unlimited.

ROME AIR DEVELOPMENT CENTER
AIR FORCE SYSTEMS COMMAND
GRIFFISS AIR FORCE BASE, NEW YORK 13441

This report has been reviewed by the RADC Information Office (01) and is releasable to the National Technical Service (NTIS). At NTIS it will be releasable to the general public, including foreign nations.

This technical report has been reviewed and approved for publication.

APPROVED:

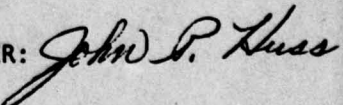


JOHN K. SCHINDLER
Acting Chief
Antenna and Radar Technique Branch

APPROVED:



ALLAN C. SCELL
Acting Chief
Electromagnetic Sciences Division

FOR THE COMMANDER: 

Plans Office

Unclassified

SECURITY CLASSIFICATION OF THIS PAGE (When Data Entered)

REPORT DOCUMENTATION PAGE			READ INSTRUCTIONS BEFORE COMPLETING FORM
1. REPORT NUMBER RADC-TR-77-250	2. GOVT ACCESSION NO.	3. PECIENT'S CATALOG NUMBER	
4. TITLE (and subtitle) DIAGNOSTIC USE OF LIQUID CRYSTAL DETECTORS IN MICROSTRIP ANTENNA DESIGN		5. TYPE OF REPORT & PERIOD COVERED Inhouse	
6. AUTHOR(s) John McIlvenna Nicholas Kernweis		7. CONTRACT OR GRANT NUMBER(s) ⑩ 14	
8. PERFORMING ORGANIZATION NAME AND ADDRESS Deputy for Electronic Technology (RADC) Hanscom AFB Massachusetts 01731		9. PROGRAM ELEMENT, PROJECT, TASK AREA & WORK UNIT NUMBERS ⑯ 62702F. 46001402	
10. CONTROLLING OFFICE NAME AND ADDRESS Deputy for Electronic Technology (RADC) Hanscom AFB Massachusetts 01731		11. REPORT DATE ⑪ July 1977	
12. MONITORING AGENCY NAME & ADDRESS (if different from Controlling Office) ⑨ Technical rpt.,		13. NUMBER OF PAGES 27	
14. DISTRIBUTION STATEMENT (of this Report) Approved for public release; distribution unlimited.		15. SECURITY CLASS. (of this report) Unclassified	
16. DISTRIBUTION STATEMENT (of the abstract entered in Block 20, if different from Report)		15a. DECLASSIFICATION/DOWNGRADING SCHEDULE ⑫ 28P.	
17. SUPPLEMENTARY NOTES			
18. KEY WORDS (Continue on reverse side if necessary and identify by block number) Microstrip antenna Circular disc resonator Liquid crystal detector Microstrip array Circular disc antenna Electromagnetic modes			
19. ABSTRACT (Continue on reverse side if necessary and identify by block number) Liquid crystal detector sheets can be used to visually display the field structure on and around planar antenna structures such as microstrip patch elements and arrays. The display aids in diagnosing feed placement problems in single elements, and pinpoints mismatch and asymmetries in array feeds. The loading effects of the detector sheets is examined and found to be of no serious consequence.			

DD FORM 1 JAN 73 1473 EDITION OF 1 NOV 65 IS OBSOLETE

Unclassified

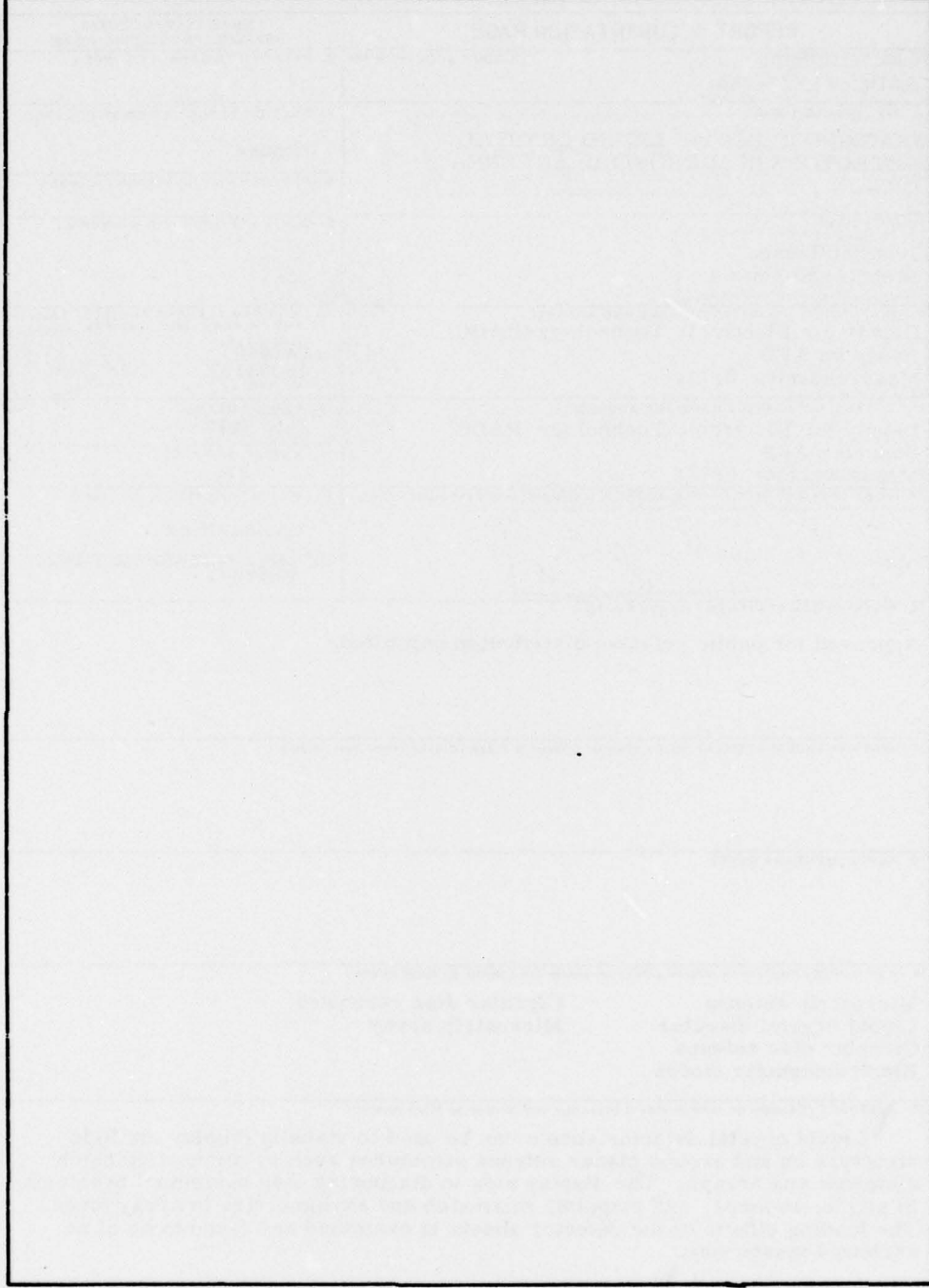
SECURITY CLASSIFICATION OF THIS PAGE (When Data Entered)

309 050

2

mt

SECURITY CLASSIFICATION OF THIS PAGE(When Data Entered)



SECURITY CLASSIFICATION OF THIS PAGE(When Data Entered)

b6
b7c

Preface

The authors express their appreciation to Dr. Robert Mailloux, RADC/ET, for the helpful discussion of several points in this paper.

ACCESSION FOR	
1 S	White Section <input checked="" type="checkbox"/>
006	Blue Section <input type="checkbox"/>
ARMED FORCES	
J. S. 111111	
PV	
DISTRIBUTION/MATURITY CODES	
SPECIAL	
A	

*NOT
Preceding Page BLANK - FILMED*

Contents

1. BACKGROUND	7
2. RESONANT MODE BEHAVIOR OF SINGLE ELEMENTS	10
3. LIQUID CRYSTAL DETECTOR DIAGNOSIS OF A MICROSTRIP ARRAY	18
4. CONCLUSIONS	20
REFERENCES	21
APPENDIX A. Loading Effects	23

Illustrations

1. S-Band Microstrip Disc Antenna and Liquid Crystal Detector in Flat Mount	9
2. Network Analyzer Display for Disc Antenna With Feed 0.56 cm From Center	11
3. E-Field Dominant Mode Structure on Disc Antenna With Feed 0.56 cm From Center (2.8 GHz)	12
4. First Higher Order Mode Structure on Disc Antenna With Feed 0.56 cm From Center (4.7 GHz)	13
5. Second Higher Order Mode Structure on Disc Antenna With Feed 0.56 cm From Center (6.5 GHz)	14

Illustrations

6. Second Higher Order Mode Structure on Disc Antenna With Feed 0.28 cm From Center (6.5 GHz)	15
7. Network Analyzer Display for Disc Antenna With Feed 0.28 cm From Center	16
8. Octagonal Mode Structure Observed on Disc Antenna at 8.2 GHz	17
9. Eight-Element, X-Band, Microstrip Array	19
10. Network Analyzer Display of Eight-Element Array, 8.5 to 9.5 GHz	20
A1. Network Analyzer Display for Disc Antenna in Dominant Mode	25
A2. Network Analyzer Display for Disc Antenna in Dominant Mode	25
A3. Network Analyzer Display for Eight-Element Microstrip Array	26
A4. Network Analyzer Display for Eight-Element Microstrip Array	26

Diagnostic Use of Liquid Crystal Detectors in Microstrip Antenna Design

I. BACKGROUND

Microstrip patch antennas offer a practical solution to many of the problems associated with low cost, lightweight, flush-mounted antennas. Single elements and arrays of microstrip patches are currently used in missile, satellite, and aircraft antenna applications.¹⁻¹⁰ Design techniques for this type of antenna are generally empirical, although simple element geometries — such as circular, square, and rectangular patches — can be partially analyzed either by modeling the elements as two radiating slots separated by a length of low loss transmission line,^{2, 11} or by treating the elements as simple dielectric cavities.¹² In the latter case, the electromagnetic modes (set up in the cavity formed by the conducting patch, dielectric, and conducting ground plane) and their respective resonant frequencies are functions of the dimensions of the patch, the thickness of the dielectric, and the dielectric constant. The frequencies predicted from simple cavity theory are only approximately realized in practice,² that is, theory and experiment agree to within about 5 percent, but modifications to the basic resonant frequency relations can improve the agreement.^{13, 14}

(Received for publication 1 August 1977)

Due to the large number of references cited above, they will not be footnoted here.
See references, page 21.

However, other aspects of microstrip patch antenna design such as the feed placement and the location of shorting pins (both of which affect the mode structure on single elements), are usually determined experimentally.² Since the mode structure is so closely related to the circuit and radiating properties of the individual element and also because each of the separate modes exhibits varied radiation patterns,² a technique that monitors mode changes as antenna patch parameters are experimentally varied, is a useful tool for the designer. A network analyzer can of course be used to investigate impedance and VSWR changes as a function of frequency. However, it is difficult to determine whether the desired mode is actually excited on the microstrip patch at a particular frequency for a given feed placement and location of shorting pins. Arrays of microstrip patch antennas present similar problems for each element and, in addition, offer the design complications of power dividers, feed lines, and element amplitude weighting. One relatively simple diagnostic method that allows the designer to see the mode structure and the field distributions on individual elements, and to monitor element excitation, feed line radiation and power divider asymmetries in arrays, uses microwave liquid crystal detectors. This technique makes it possible for the designer to actually watch mode and field structure changes as he experimentally varies the element or array parameters. Resistive backed cholesteric liquid crystal^{*} sheets convert microwave energy into visual patterns and have been used to display the electric and magnetic standing wave mode distributions on various microwave devices.^{15, 16}

Microstrip antennas and liquid crystal devices work well together in the laboratory. The antennas are usually small, conducting patches on flat dielectric boards. The resistively backed liquid crystal (in a lightweight, nonconducting frame) can simply be placed directly over the antenna. (See discussion of loading in Appendix A.) The resultant display can be used to deduce the electric and magnetic field geometry. The variation in the colors of the display is directly related to gradients in field intensity over the surface of the antenna. The crystal display continuously monitors, in real time, the resonant mode structural and intensity changes as the element feed position is altered or the feed line geometry is changed. Since the crystal provides a display at any microwave frequency, the designer can simply sweep through all the frequencies of interest while watching both the variations in the field structure and the transitions from mode to mode. The designer

*The authors are indebted to Mr. James Sethares of RADC/ET for the use of his liquid crystal detectors.

15. Sethares, J., and Gulaya, S. (1970) Visual observation of rf magnetic fields using cholesteric liquid crystals, Applied Optics, p 2795.
16. Sethares, J., and Stiglitz, M. (1969) Visual observation of high dielectric resonator modes, Applied Optics, p 2560.

can obtain crude but useful indications of bandwidth by simply noting the frequencies at which a mode structure appears and disappears, and he can also monitor the impedance match between feed line and antenna by noting the intensity of the display colors as the feed position is varied.

The liquid crystal detectors make comparisons between individual elements in an array a simple matter. The detection of fabrication or excitation flaws is as simple as comparing the crystal display from element to element. In a sense, the crystal detectors provide in a single integrated view, all the amplitude or power information picked up sequentially (and then recorded) by a very wideband near-field probe.

Using the liquid crystal detectors requires no special laboratory apparatus other than the crystals themselves. Figure 1 shows an S-band microstrip antenna and the liquid crystal detector. A biasing lamp can be used to raise the temperature of the crystals to the point where very weak fields can be detected.¹⁵ This

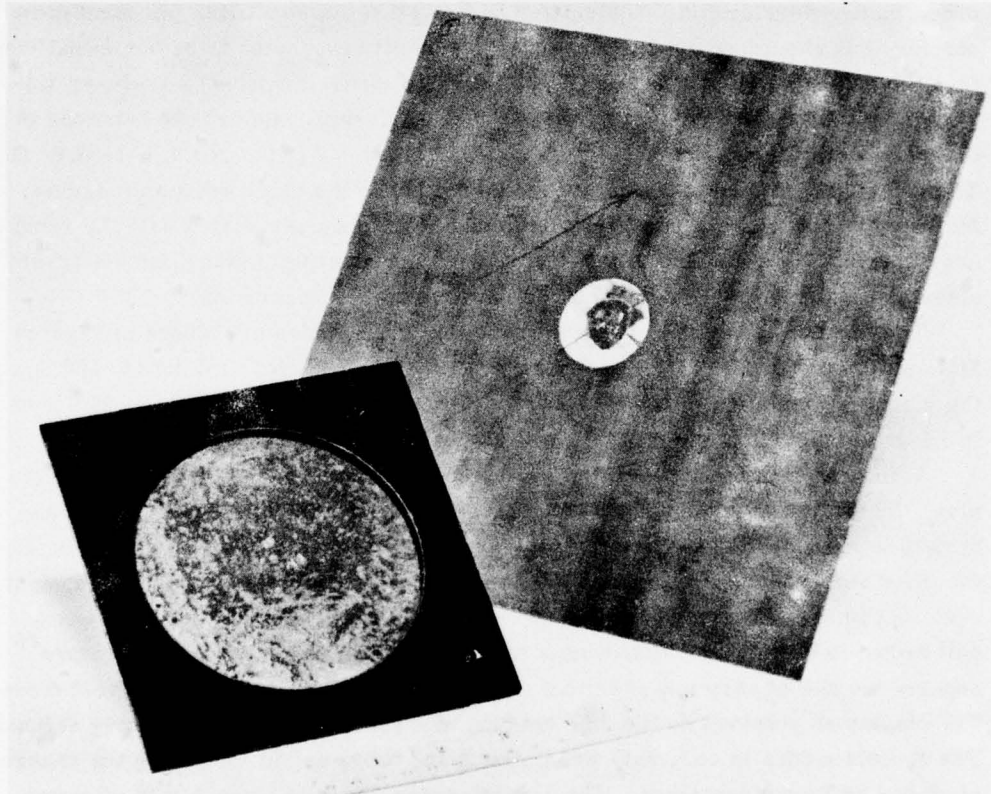


Figure 1. S-Band Microstrip Disc Antenna and Liquid Crystal Detector in Flat Mount

was not found to be necessary in any of the experiments described in this article. The versatility and usefulness of the liquid crystal detectors in diagnosing mode structure problems in single microstrip elements and verifying the design performance of an array of microstrip elements, is described in the following sections.

2. RESONANT MODE BEHAVIOR OF SINGLE ELEMENTS

A circular disc element was fabricated from 1/16-in. double clad teflon-fiberglass board material ($\epsilon_R = 2.55$). A mode suppressing pin² was inserted at the disc center and the feed was placed on the back of the disc at a 50Ω point, found by experiment to be about 0.559 cm from the center. Using the standard resonant frequency relations available in the literature,² the calculated frequency for the dominant mode of the 1.83 cm radius disc was 3 GHz. The next two higher order modes were similarly calculated to lie at 4.7 and 6.5 GHz. As mentioned earlier, one should expect the measured resonant frequencies to be somewhat less than the values calculated. Figures 2(a) and 2(b) show the network analyzer display for the disc element over the 2.6 to 8.0 GHz range. Resonance behavior is indicated in three regions, 2.79 to 2.82 GHz, about 4.7 GHz, and 6.47 to 6.67 GHz. The designer would be justified in concluding that in the three resonant regions indicated on the network analyzer, the mode structures associated with the resonance frequencies would actually be excited on the microstrip disc. Liquid crystal detectors make it possible to check the validity of this conclusion.

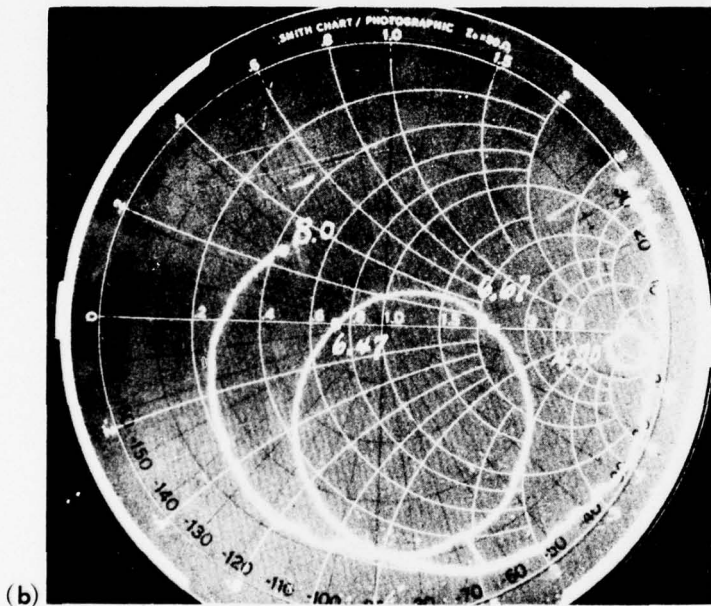
The theoretical E-field structures for the three modes are shown in Figures 3(a), 4(a), and 5(a).¹⁷ Using liquid crystals with a resistive backing of $1100 \Omega/\text{sq.}$, the visual presentation of the E-field modes actually present on the disc is shown in Figures 3(b), 4(b), and 5(b).

In interpreting these black and white reproductions of the detector color display, the reader should envision the region inside the crescent shaped areas as dark blue in color. These are the regions of intense fields. The lighter halo about the crescents is actually composed of two colors, bright green closest to the crescent, becoming dull orange further out. The remainder of the photo area has a dull brown to black color indicating a lack of field components. The literature¹⁵ reports the use of very low resistive coatings to visually display the H-field modes. The display so obtained on the disc antenna was relatively weak and poorly defined. The E-field modes in contrast, were strong and more useful for noting the changes produced by feed placements. The crystals were run with about 1.0 W of power from a TWT.

17. Watkins, J. (1969) Circular resonant structures in microstrip, Electronic Letters 5:(No. 21).



(a)



(b)

Figure 2. Network Analyzer Display for Disc Antenna With Feed 0.56 cm From Center. (a) 2.6 to 3.2 GHz; and (b) 4.0 to 8.0 GHz

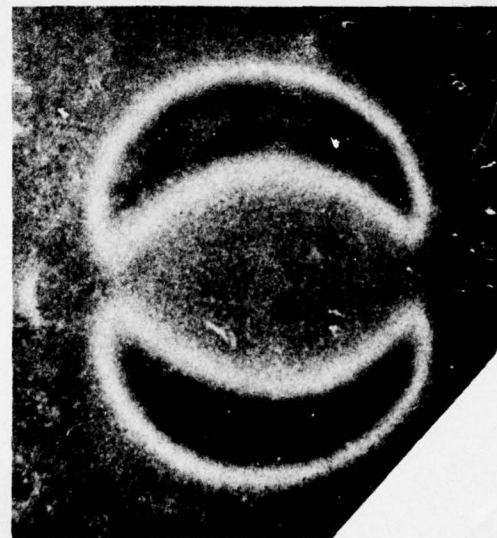
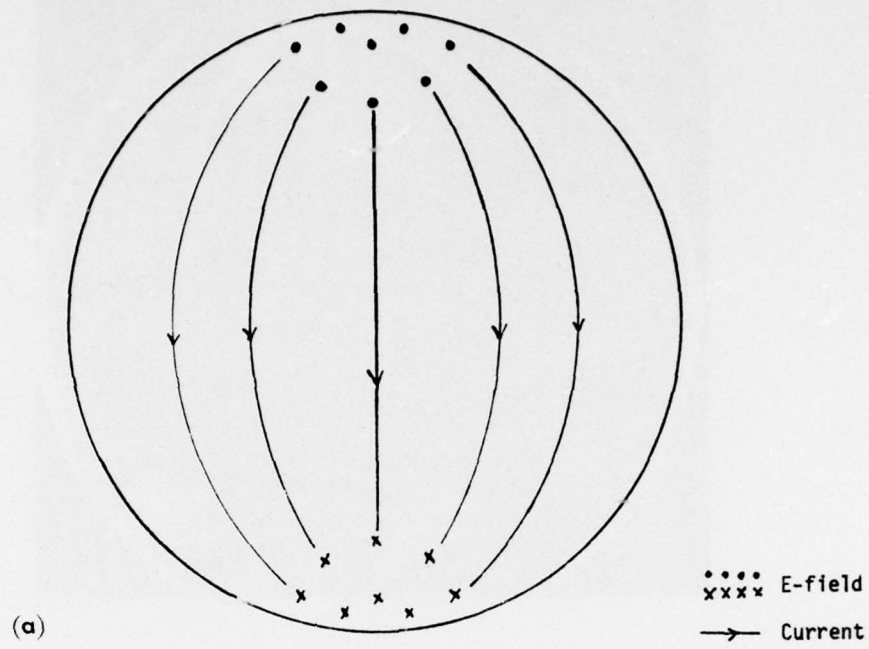


Figure 3. E-Field Dominant Mode Structure on Disc Antenna With Feed 0.56 cm From Center (2.8 GHz). (a) Calculated from mode theory; and (b) observed with liquid crystal

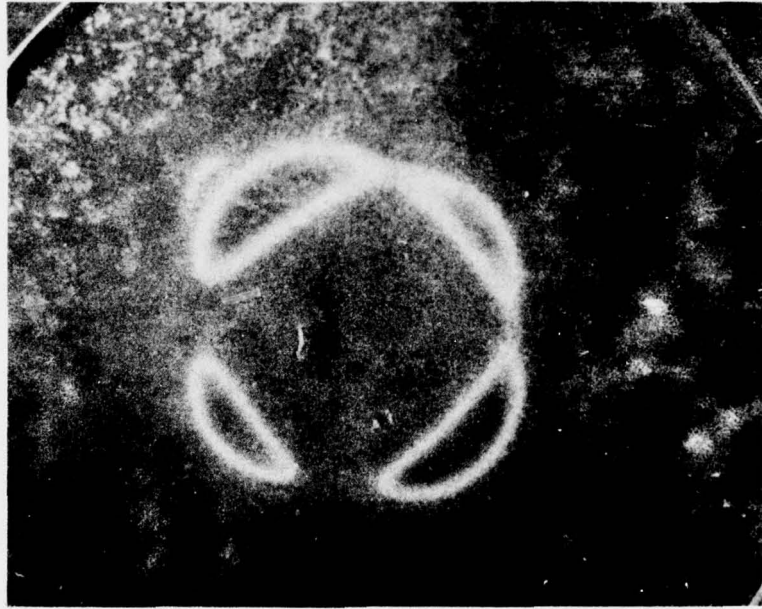
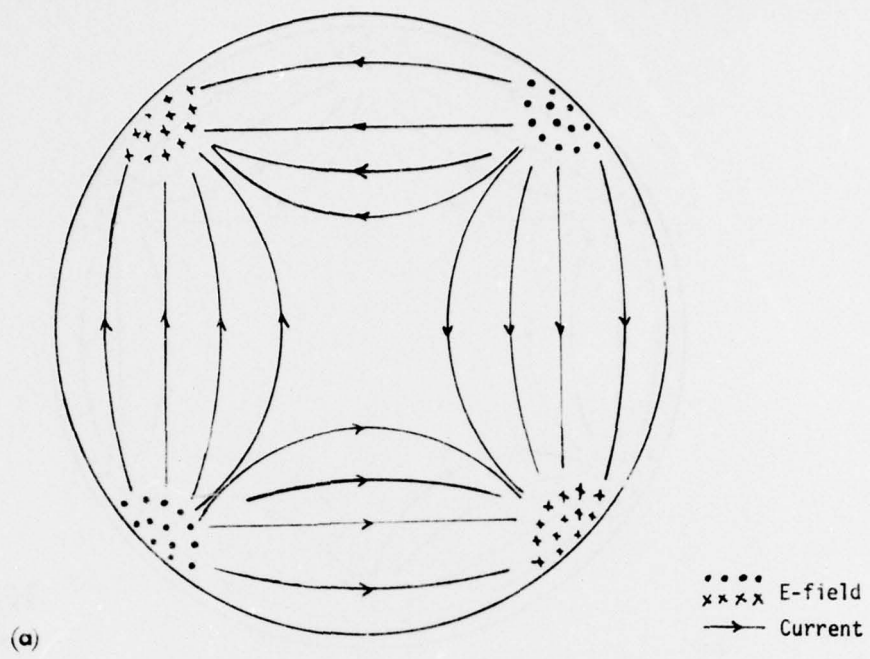


Figure 4. First Higher Order Mode Structure on Disc Antenna With Feed 0.56 cm From Center (4.7 GHz). (a) Calculated; and (b) observed

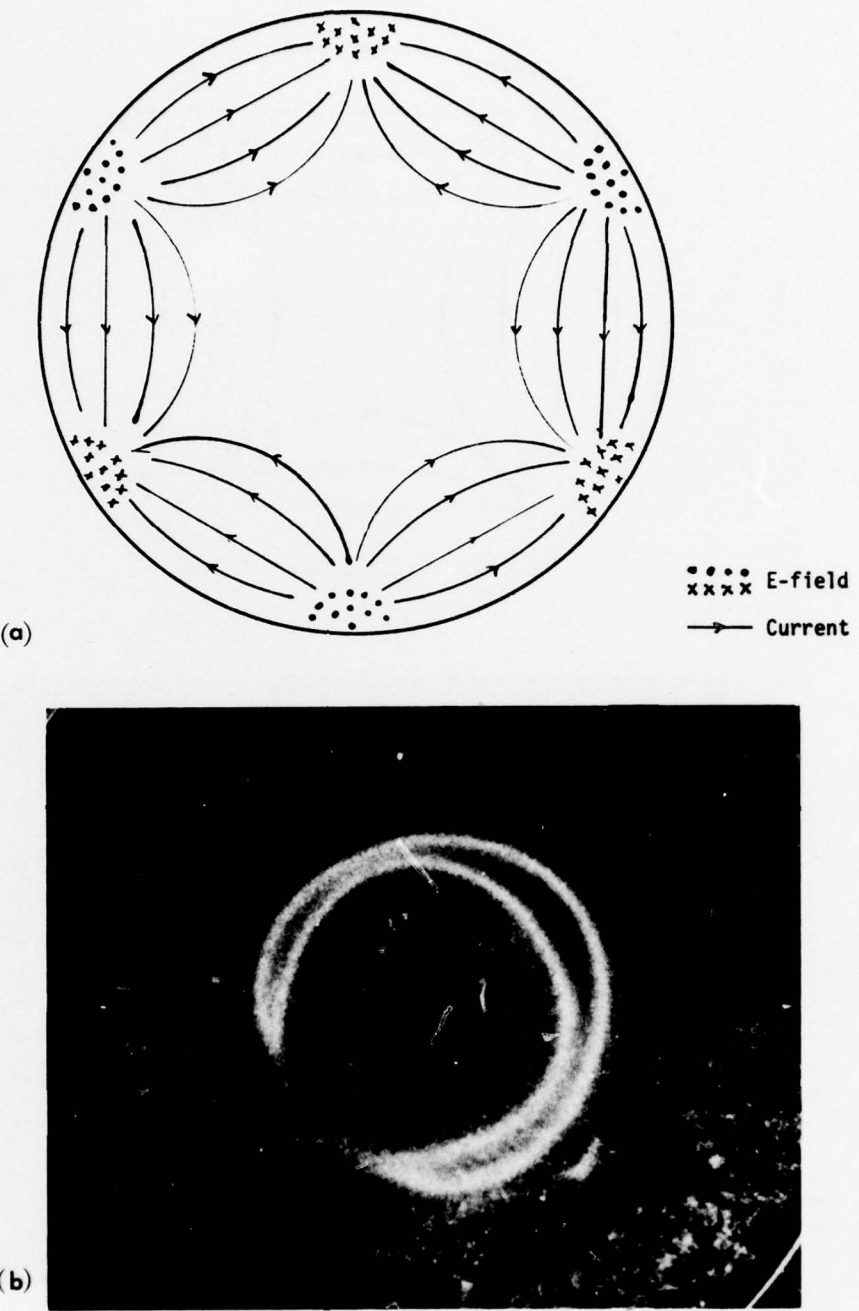


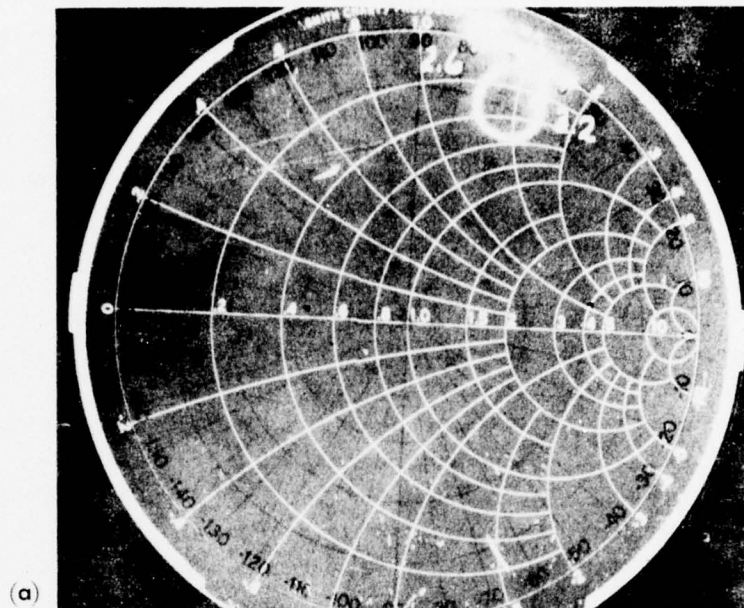
Figure 5. Second Higher Order Mode Structure on Disc Antenna With Feed 0.56 cm From Center (6.5 GHz). (a) Calculated; and (b) observed

Note that Figure 3 shows good agreement between the predicted and measured dominant mode patterns. Although Figure 4(b) is easily recognized as the four-sided mode structure of Figure 4(a), there is some asymmetry in the visual display indicating that the feed placement is not quite optimum for this mode. Figure 5(b) indicates that the hexagon shaped mode structure predicted at 6.5 GHz is, in fact, not excited. The location of the feed at 0.559 cm, although optimum for the dominant mode and acceptable for the first mode, is completely unsatisfactory for this second mode. The visual display of Figure 5(b) shows what the network analyzer can not; that is, although the disc is resonant at about 6.5 GHz, the resonance is not the expected mode structure. A sweep through the 2 to 10 GHz range using the crystal detector showed that the hexagon shaped mode was never excited with the feed placed at 0.559 cm.

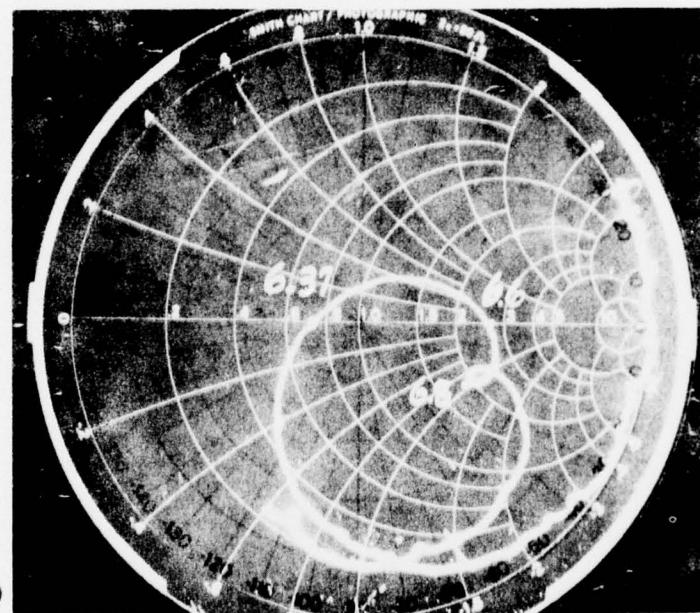
Using the liquid crystal display as a guide, the feed was systematically repositioned and eventually placed at a distance of 0.279 cm from the center. Figure 6 shows that this new feed location does indeed excite the disc into the hexagon shaped mode predicted by theory. Of course, the altered feed position produces changes in the dominant and first mode behavior. Figures 7(a) and (b) show the network analyzer trace of the disc with the feed moved to its new location at 0.279 cm.



Figure 6. Second Higher Order Mode Structure on Disc Antenna With Feed 0.28 cm From Center (6.5 GHz)



(a)



(b)

Figure 7. Network Analyzer Display for Disc Antenna With Feed 0.28 cm From Center. (a) 2.6 to 3.2 GHz; and (b) 4.0 to 8.0 GHz

The liquid crystal display over this same frequency range was used to verify that the new feed position produced a substantially weaker dominant mode and failed entirely to excite the four-sided mode at 4.7 GHz. Thus, the crystal detectors prove to be effective diagnostic aids in experimentally determining the relation between the feed position and the mode structure excited on the microstrip element. Figure 8 shows an even higher order, eight-sided mode structure at 8.2 GHz.

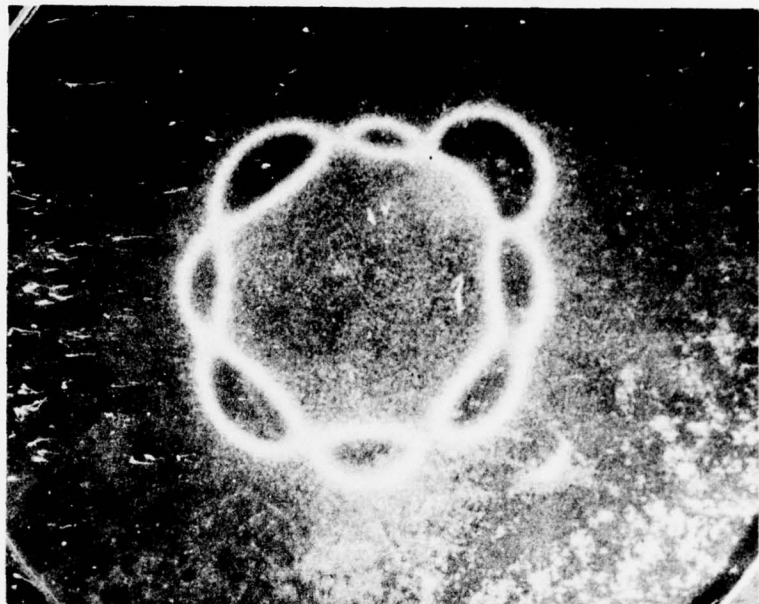


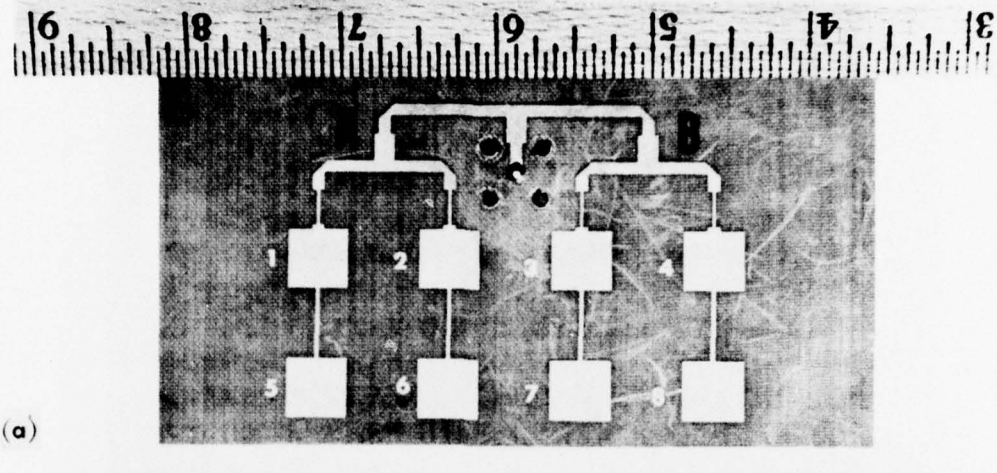
Figure 8. Octagonal Mode Structure Observed on Disc Antenna at 8.2 GHz

The crystals proved useful in a variety of other microstrip fabrication related problems. Loosened or poor solder connections were often detected because of weak crystal displays. Microstrip patches fabricated by different processes could be compared via their crystal displays. The crystals also showed that as frequency is varied over a broad range, say 2 to 10 GHz, the microstrip patch element produces a variety of distinctive field configurations in addition to its resonance modes. Many of these field patterns are antisymmetric and not predicted by a modal analysis.

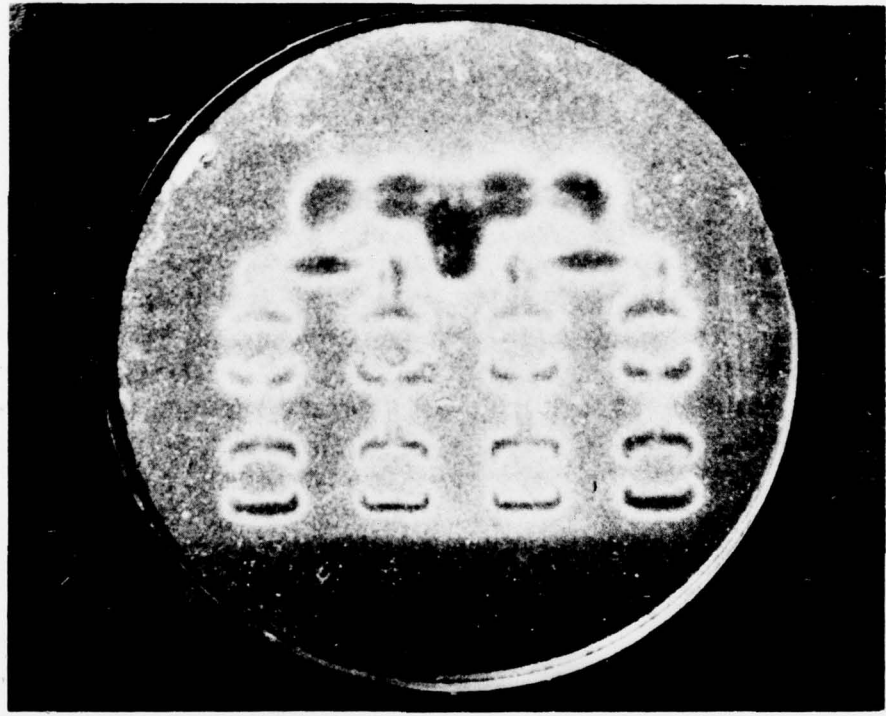
3. LIQUID CRYSTAL DETECTOR DIAGNOSIS OF A MICROSTRIP ARRAY

Figure 9(a) shows an 8-element, two row microstrip array with matching transformers, power dividers, and single point feed.* The square elements are center fed at one edge and designed to be equally excited in their dominant mode at 9 GHz. Figure 10 shows the network analyzer trace of the array over the 8.5 to 9.5 GHz frequency range. Figure 9(b) shows the liquid crystal display for the array at 8.85 GHz. Several aspects of the design are apparent in this presentation. Note first of all, the indication of intense fields on the lines between the feed point, points A and B, and the top row elements. There is obviously substantial energy in the form of standing waves on these lines. There is, in addition, a slight asymmetry in the power division at points A and B. It can also be seen that the elements are not equally excited. In general, the bottom row elements have more intense edge fields than the top row elements. Three of the outer elements, that is, 4, 5 and 8, have stronger fields than the other elements. Element 1 appears the weakest. The feed lines between elements 2 and 6 and between 3 and 7 can be seen to have higher standing waves than the other inter-row feed lines. This one array example shows that the liquid crystal display provides a variety of diagnostic information not available from the network analyzer which can aid the designer in pinpointing trouble spots in his feed and power distribution network.

*The array was supplied by Dr. Anders Derneryd, RADC/ET Visiting Scientist. Subsequent to the use of the crystal detectors by the authors, Dr. Derneryd made use of them in analyzing the rectangular microstrip element and reported these results in A Theoretical Investigation of the Rectangular Microstrip Antenna Element, presented at the 1977 AP-URSI Conference in San Francisco.



(a)



(b)

Figure 9. Eight-Element, X-Band, Microstrip Array. (a) Actual array; and (b) liquid crystal display at 8.85 GHz

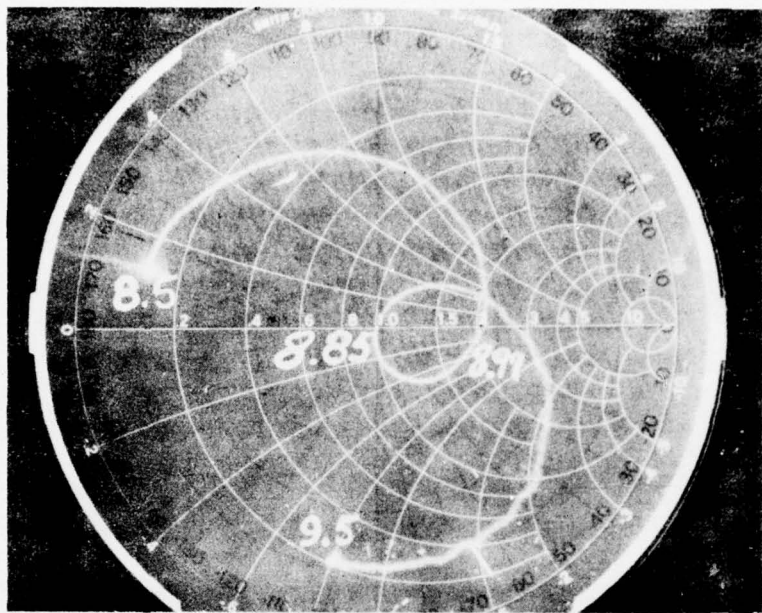


Figure 10. Network Analyzer Display of Eight-Element Array,
8.5 to 9.5 GHz

4. CONCLUSIONS

Liquid crystal detectors provide a real time, simple diagnostic capability for microstrip circuits, radiating elements, and arrays. They provide a type of visual information not available from network analyzers and in addition, require little in the way of laboratory equipment. Usable at any frequency, the detectors represent a sensible test device for operations that range from laboratory development to the production line testing and comparison of manufactured units.

References

1. Waterman, A., and Henry, D. (1971) Stripline Strap-On Antenna Array, 21st USAF Antenna Symposium, Monticello, Ill.
2. Howell, J.Q. (1975) Microstrip antennas, IEEE Trans. AP:90-93.
3. Weinschel, D. (1975) A cylindrical array of circularly polarized microstrip antennas, 1975 AP-S International Symposium Record, p 177.
4. Munson, R. (1974) Conformal microstrip antennas and microstrip phased arrays, IEEE Trans. AP:74-78.
5. Sanford, G. (1974) Conformal Microstrip Phased Array for Aircraft Tests with ATS-6, Proc. Natl. Elec. Conference, Vol. 29.
6. Brain, D., and Mark, J. (1973) The disc antenna - a possible L-band aircraft antenna, Intl. Conf. on Satellite Systems for Mobile Comm. and Surveillance, London.
7. Garvin, C., et al (1975) Low profile electronically small missile base mounted microstrip antennas, 1975 G-AP Symposium Record, p 244.
8. Laughlin, G. (1975) Wideband Solid State Phased Array Antenna Development at VHF, John Hopkins University Report TG-1278.
9. Munson, R., et al (1976) Microstrip Communications Antenna, Final Report, RAD-C-TR-76-147.
10. Greiser, J. (1976) Co-planar stripline antenna, Microwave Journal, p 47.
11. Derneryd, A. (1976) Linearly polarized microstrip antennas, IEEE Trans. AP, p 846.
12. Long, S., and Shen, L. (1976) An experimental and theoretical investigation of the circular disc printed circuit antenna, Proc. ECOM-ARO Workshop on Electrically Small Antennas, Ft. Monmouth, N.J.
13. Kaloi, C. (1975) Asymmetrically Fed Electric Microstrip Dipole Antenna, TP-75-03, Naval Missile Center, Point Magu, CA.

14. Black, L., and McCorkle, J. (1975) A Preliminary Report on the Inhouse Exploratory Development Program on Microstrip Patch Antennas at the Naval Surface Weapons Center, NSWC-WOL-TR-75-200.
15. Sethares, J., and Gulaya, S. (1970) Visual observation of rf magnetic fields using cholesteric liquid crystals, Applied Optics, p 2795.
16. Sethares, J., and Stiglitz, M. (1969) Visual observation of high dielectric resonator modes, Applied Optics, p 2560.
17. Watkins, J. (1969) Circular resonant structures in microstrip, Electronic Letters 5:(No. 21).

Appendix A

Loading Effects

A resistively backed liquid crystal detector placed in proximity to a radiating device — such as the microstrip antennas discussed in this article — produces a loading effect that depends both on the resistivity of the detector backing and the height of the detector sheet above the antenna. Generally speaking, the higher the resistivity and the greater the separation between the antenna and the crystal detector, the smaller the loading effect. A question arises as to whether the detector loading significantly alters the field distribution on the element under test. The network analyzer proves useful in quantifying these effects.

Figure A1 shows network analyzer traces of a simple disc element over a frequency range that includes its dominant mode. Curve A is the trace of the isolated element. Curve B shows the change produced when a liquid crystal detector with resistivity of 8.5 K Ω /sq. is placed 4 mm above the disc. Curve C represents the case when the detector is 2 mm above the antenna and Curve D illustrates the maximum loading produced when the detector lies directly atop the antenna. Note that the loading causes a small change in impedance value at almost all frequencies displayed, the change being greatest at the disc resonant frequency. The resonant frequency itself, however, changes only about 0.4 percent (from 2.798 GHz to 2.786 GHz) with loading. The actual crystal display is bright and sharp with the detector atop the disc and, as should be expected, loses some intensity and edge definition as the separation increases to 8 mm. At any stage, however, the characteristic dominant mode field structure is clearly defined and the intensity

distribution on the detector face does not appear to be a sensitive function of the separation between disc and detector.

Figure A2 shows the same situations except a detector with $1100 \Omega/\text{sq}$ is used. The impedance change with loading is more pronounced but again, the resonant frequency shifts only about 0.4 percent. The detector displays are brighter than those of the $8.5 \Omega/\text{sq}$ detector and they too are seemingly insensitive to detector-disc separation distances.

Figures A3 and A4 show the maximum loading effect of the two detectors on the X-band array of Figure 9(a). Trace A in both figures represents the isolated array, Trace B of Figure A3 corresponds to the $8.5 \text{ K}\Omega/\text{sq}$ detector placed atop the array, while Trace B of Figure A4 represents the $1100 \Omega/\text{sq}$ detector placed directly on top of the array. Both figures show impedance changes and a shift in frequency of 0.4 percent and 1.7 percent for the $8.5 \text{ K}\Omega/\text{sq}$ and $1100 \Omega/\text{sq}$ detectors, respectively.

In general, as the detector is lowered from above to the vicinity of the antenna under test there are a number of distances that occur periodically, at which the loading effect is minimal or nondiscernible; that is, the network analyzer trace shows little or no change when the detector is in place over the antenna. For example, with a resistivity of $8.5 \text{ K}\Omega/\text{sq}$, the closest that the detector can be placed above the antenna with no discernible loading is 0.55 cm, while for the $1100 \Omega/\text{sq}$ detector, the corresponding distance is 0.75 cm. At these separating distances, however, the crystal displays, being washed out and fuzzy, are not very useful for diagnostic purposes.

Placing the detector sheet directly on top of the antenna under test is the simplest laboratory diagnostic method. The small changes in frequency due to the loading indicate that the crystal has not induced any mode variations that could be associated with a change in field geometry. Adding the observation that the detector display remains basically unchanged as the detector is moved away from the test antenna, one can conclude that loading effects — especially with the high resistivity backing — are not a limiting factor on the use of the crystals as mode and intensity detectors. However, as can be seen from Figures A1-A4, impedance and bandwidth design problems are sensitive functions of the loading and require careful consideration.

Although such observations do not constitute formal proof that loading effects are unimportant, the designer can feel that simply placing the detector on top of the microstrip antenna is a usable method that provides him with the essential distribution of fields on the device under test. Other experiments with liquid crystal detectors on nonradiating devices such as two wire lines, a single wire above a groundplane, microstrip lines, and high dielectric resonators, have also led to the

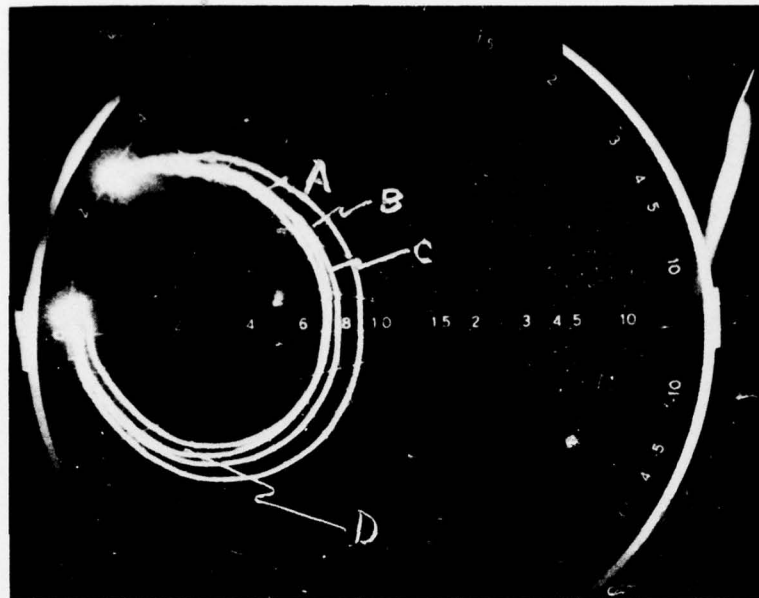


Figure A1. Network Analyzer Display for Disc Antenna in Dominant Mode.
A. Isolated disc, B. $8.5 \text{ K}\Omega/\text{sq}$ detector 4 mm above disc, C. $8.5 \text{ K}\Omega/\text{sq}$ detector 2 mm above disc, and D. $8.5 \text{ K}\Omega/\text{sq}$ detector on top of disc

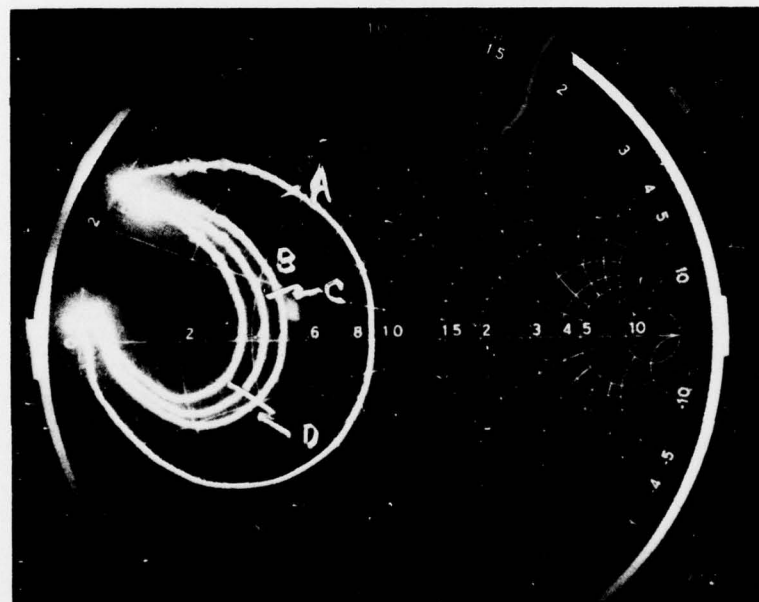


Figure A2. Network Analyzer Display for Disc Antenna in Dominant Mode.
A. Isolated antenna, B. $1100 \Omega/\text{sq}$ detector 4 mm above disc, C. $1100 \Omega/\text{sq}$ detector 2 mm above disc, and D. $1100 \Omega/\text{sq}$ detector on top of disc

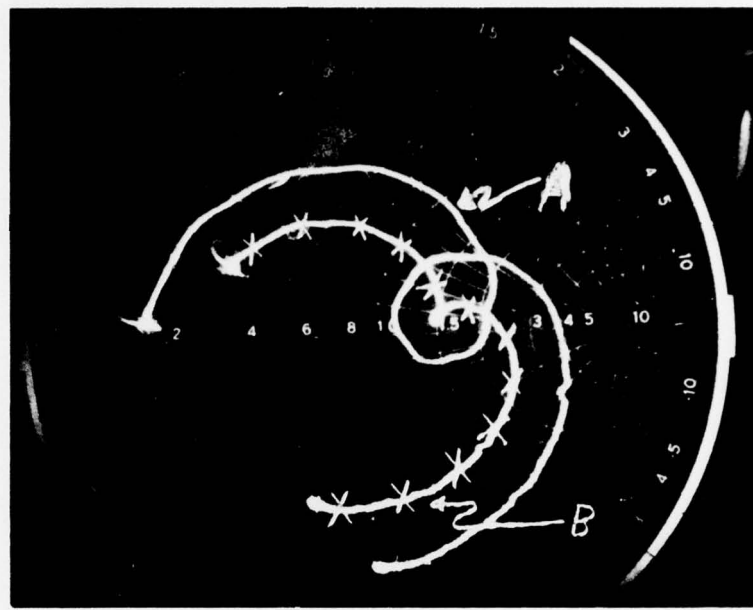


Figure A3. Network Analyzer Display for Eight-Element Microstrip Array. A. Isolated array, and B. $8.5 \text{ K}\Omega/\text{sq}$ detector on top of array

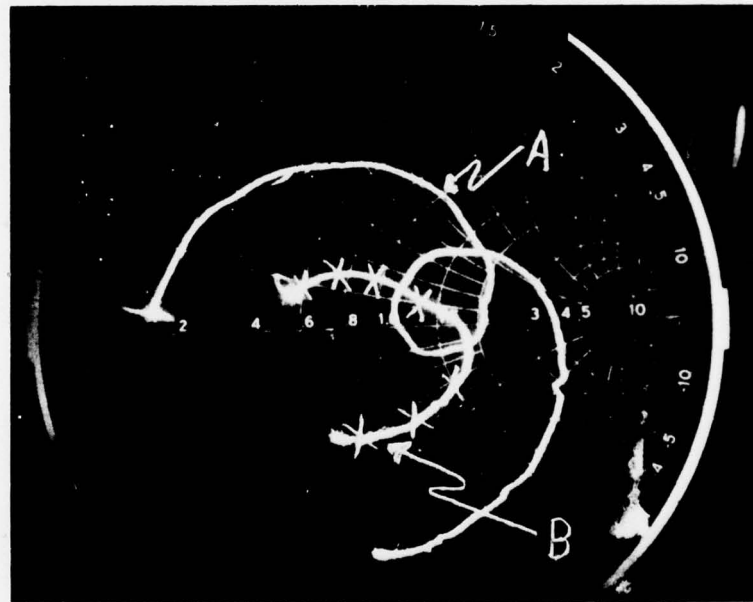


Figure A4. Network Analyzer Display for Eight-Element Microstrip Array. A. Isolated array, and B. $1100 \Omega/\text{sq}$ detector on top of array

the conclusion that the observed field patterns are relatively insensitive to the separation between the detector and the physical structure.*

* J. C. Sethares, Deputy for Electronic Technology. Private Communication.

METRIC SYSTEM

BASE UNITS:

Quantity	Unit	SI Symbol	Formula
length	metre	m	...
mass	kilogram	kg	...
time	second	s	...
electric current	ampere	A	...
thermodynamic temperature	kelvin	K	...
amount of substance	mole	mol	...
luminous intensity	candela	cd	...

SUPPLEMENTARY UNITS:

plane angle	radian	rad	...
solid angle	steradian	sr	...

DERIVED UNITS:

Acceleration	metre per second squared	...	m/s
activity (of a radioactive source)	disintegration per second	...	(disintegration)/s
angular acceleration	radian per second squared	...	rad/s
angular velocity	radian per second	...	rad/s
area	square metre	...	m
density	kilogram per cubic metre	...	kg/m ³
electric capacitance	farad	F	A·s/V
electrical conductance	siemens	S	A/V
electric field strength	volt per metre	...	V/m
electric inductance	henry	H	V·s/A
electric potential difference	volt	V	W/A
electric resistance	ohm	Ω	V/A
electromotive force	volt	V	W/A
energy	joule	J	N·m
entropy	joule per kelvin	...	J/K
force	newton	N	kg·m/s
frequency	hertz	Hz	(cycle)s
illuminance	lux	lx	lm/m ²
luminance	candela per square metre	...	cd/m ²
luminous flux	lumen	lm	cd·sr
magnetic field strength	ampere per metre	...	A/m
magnetic flux	weber	Wb	V·s
magnetic flux density	tesla	T	Wb/m ²
magnetomotive force	ampere	A	...
power	watt	W	J/s
pressure	pascal	Pa	N/m
quantity of electricity	coulomb	C	A·s
quantity of heat	joule	J	N·m
radiant intensity	watt per steradian	...	W/sr
specific heat	joule per kilogram-kelvin	...	J/kg·K
stress	pascal	Pa	N/m
thermal conductivity	watt per metre-kelvin	...	W/m·K
velocity	metre per second	...	m/s
viscosity, dynamic	pascal-second	...	Pa·s
viscosity, kinematic	square metre per second	...	m ² /s
voltage	volt	V	W/A
volume	cubic metre	...	m ³
wavenumber	reciprocal metre	...	(wave)m ⁻¹
work	joule	J	N·m

SI PREFIXES:

Multiplication Factors	Prefix	SI Symbol
$1\ 000\ 000\ 000\ 000 = 10^{12}$	tera	T
$1\ 000\ 000\ 000 = 10^9$	giga	G
$1\ 000\ 000 = 10^6$	mega	M
$1\ 000 = 10^3$	kilo	k
$100 = 10^2$	hecto	h
$10 = 10^1$	deka	d
$0.1 = 10^{-1}$	deci	d
$0.01 = 10^{-2}$	centi	c
$0.001 = 10^{-3}$	milli	m
$0.000\ 001 = 10^{-6}$	micro	μ
$0.000\ 000\ 001 = 10^{-9}$	nano	n
$0.000\ 000\ 000\ 001 = 10^{-12}$	pico	p
$0.000\ 000\ 000\ 000\ 001 = 10^{-15}$	femto	f
$0.000\ 000\ 000\ 000\ 001 = 10^{-18}$	atto	a

* To be avoided where possible.

MISSION
of
Rome Air Development Center

RADC plans and conducts research, exploratory and advanced development programs in command, control, and communications (C³) activities, and in the C³ areas of information sciences and intelligence. The principal technical mission areas are communications, electromagnetic guidance and control, surveillance of ground and aerospace objects, intelligence data collection and handling, information system technology, ionospheric propagation, solid state sciences, microwave physics and electronic reliability, maintainability and compatibility.